JOURNAL OF APPLIED ELECTROCHEMISTRY 26 (1996) 283–290

Zinc–nickel alloy electrodeposition from uncomplexed acid bath

M. PUSHPAVANAM, K. BALAKRISHNAN

Central Electrochemical Research Institute, Karaikudi 623006, India

Received 21 February 1995; revised 21 June 1995

Zinc–nickel alloys, as protective coatings, are well known and a new citrate bath has been investigated. It was observed that boric acid favoured nickel deposition playing the dual role of specific adsorption and catalysis. The voltammetric behaviour of the alloy deposition in the presence of boric acid is described. The effect of Ni/Zn ratio, and potential scan range on the cathodic and anodic portions of the voltammograms are discussed. The presence of two cathodic peaks at high Ni/Zn ratios, which disappeared at lower ratios was identified.

1. Introduction

Our previous work [1–4] has dealt with alloy deposition from a citrate based sulfate electrolyte as well as their physico-mechanical properties and corrosion resistance. During the present study it was found that boric acid addition had a profound influence in increasing the nickel content of the alloy. This paper deals with voltammetric studies on the role of boric acid in zinc–nickel alloy deposition.

2. Experimental details

Voltammetric studies were carried out in a conventional three compartment cell using a copper rod of 0.2826 cm^2 area as the working electrode, fitted in a Teflon sleeve. Platinum foil was used as the counter electrode. Potential scanning was effected using a potentiogalvanoscan (Wenking model 81) connected to a scan generator (Wenking model SG 79) and a X–Y–t recorder. Potentials were measured with respect to a saturated calomel electrode (SCE).

Electrolytes were prepared using analytical grade salts in triple distilled water and deaerated with purified nitrogen before each experiment. The effect of addition of boric acid on nickel and zinc deposition was studied in individual systems and then in combination. Cyclic voltammograms were obtained by varying the metal ion concentration, their ratio and operating conditions at $32 \pm 2\,^{\circ}C$ and at pH 3, unless otherwise stated. Experiments were also conducted by altering the switching potentials. The scan rate was generally 10 $mV\,s^{-1}$. The stripping charge was calculated by integrating current and time.

3. Results and discussion

A typical voltammogram obtained in 0.5 M sodium sulfate is shown in Fig. 1. For convenience, only the cathodic portion is given. The peak current corresponding to H^+ discharge showed a linear variation with the square root of scan rate (Fig. 2(a)) with a zero intercept, indicative of a diffusion controlled process. The diffusion current also increased with stirring of the electrolyte and with decreasing pH.

In the presence of boric acid (Fig. 1) the peak current for H^+ was slightly inhibited, due to adsorption of borate ions on the electrode surface. The overpotential for hydrogen evolution was lowered by about 200 mV.

3.1. *Nickel deposition*

When nickel solution was added to sodium sulfate electrolyte (Fig. 3), the H^+ discharge current remained unaltered as observed using low concentrations of nickel sulfate. The H^+ discharge was followed by the nickel reduction peak. It was concluded that after the diffusion limiting region of H^+ discharge the surface pH increased (i.e., $pH_s > pH_b$) and nickel discharge was facilitated through $NiOH^+$ ions formed at the electrode surface. Since in plain Na_2SO_4, the H^+ discharge continued up to -1.2 V, it may also lead to formation of nickel hydride [5]. This nickel deposit possessing a high hydrogen content (0.6%) is termed β-nickel by Fleischman *et al.* [6]. In the absence of boric acid the surface pH increased to very high values and a very low limiting current for nickel discharge was observed (Fig. 3). The deposits obtained, especially at concentrations above 0.1 M were thin and nonuniform. At high concentrations (0.6 M) better deposits were obtained but they were greyish in appearance. For nickel discharge the reaction order with respect to nickel ion was found to be +1 and that with respect to pH was 0.6 indicating the participation of both nickel and hydroxyl ions in nickel deposition. The cathodic slope was found to

0021-891X

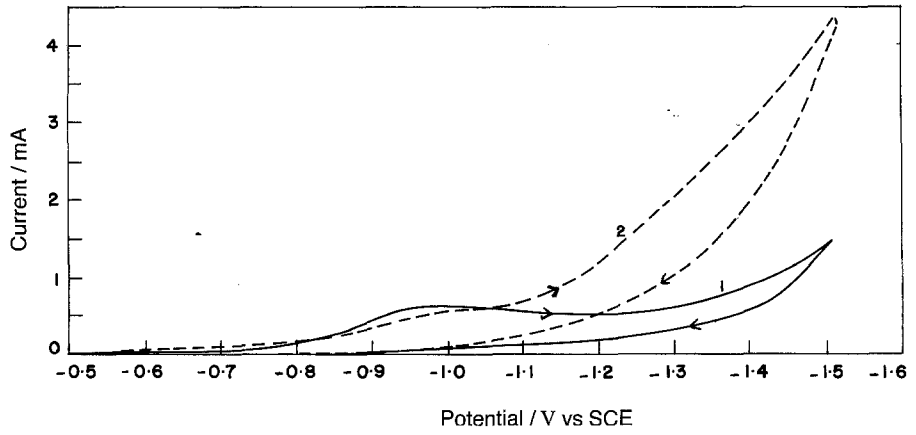

Fig. 1. CV in the blank electrolyte. (1) 0.5 M Sodium sulfate, (2) 0.5 M sodium sulfate + 0.66 M boric acid, pH 3, still condition, 50 mV/s.

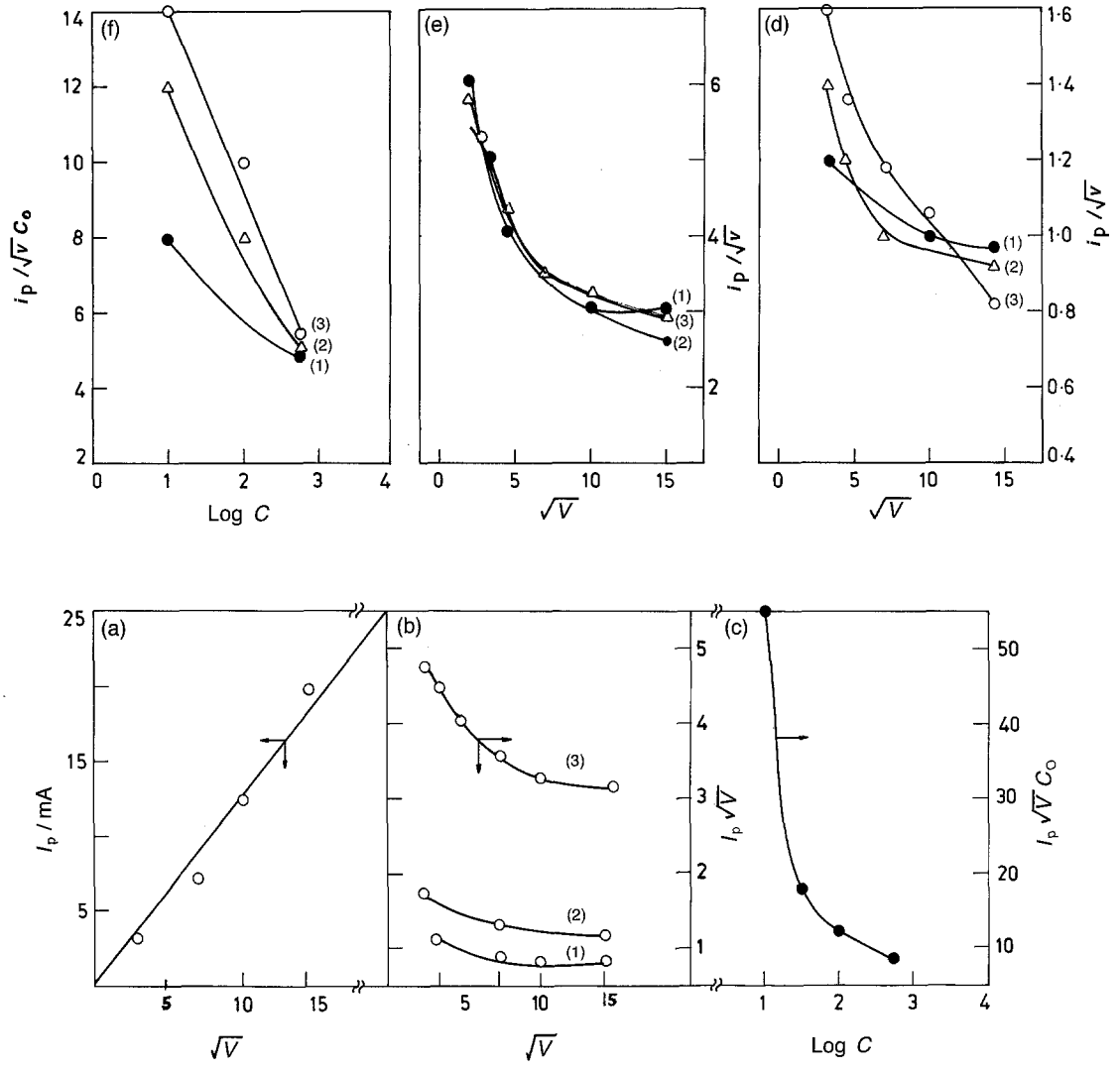

Fig. 2. (a) Variation of I_p with sweep rate for H^+ discharge reaction in 0.5 M sodium sulfate, pH 3, 50 mV s^{-1}. (b) Variation of $I_p/v^{1/2}$ with sweep rate for nickel deposition in 0.5 M sodium sulfate, 0.66 M boric acid, pH 3, Ni concentration: (1) 0.05, (2) 0.1 and (3) 0.6 M. (c) Variation of $I_p/v^{1/2}$ C_0 with concentration of nickel. Sodium sulfate 0.5 M; boric acid 0.66 M; pH 3; 50 mV s^{-1}. (d) Variation of $I_p/v^{1/2}$ with $v^{1/2}$ for zinc deposition in 0.5 M sodium sulfate, 0.66 M boric acid, 0.1 M zinc; pH: (1) 3, (2) 4 and (3) 5. (e) As above with 0.6 M zinc. (f) Variation of $I_p/v^{1/2}$ C_0 with concentration of zinc in 0.5 M sodium sulfate, 0.66 M boric acid, 100 mV s^{-1}, others as above.

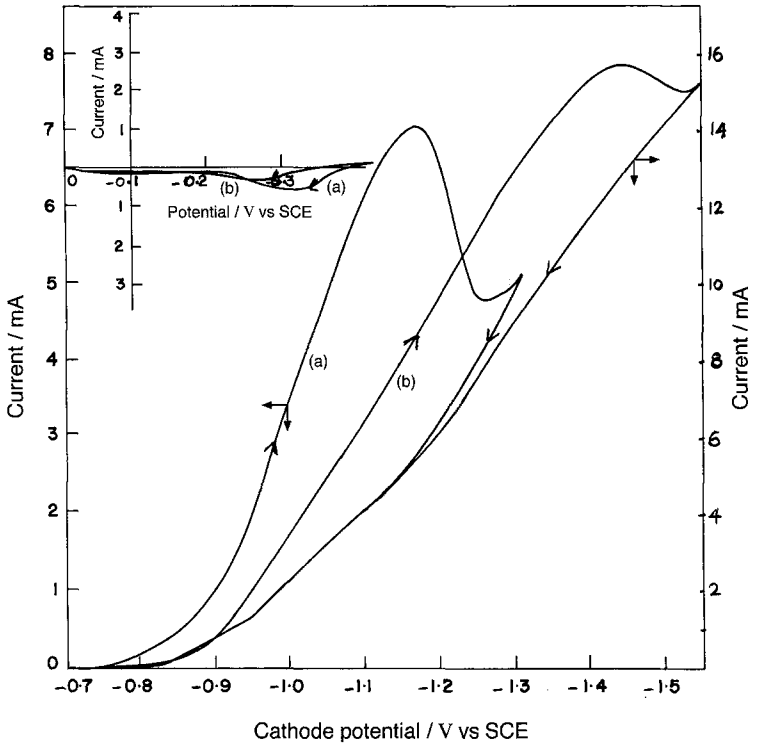

Fig. 3. CV in (a) 0.5 M sodium sulfate + 0.6 M nickel sulfate (b) 0.5 M sodium sulfate + 0.6 M nickel sulfate + 0.66 M boric acid. Insert: anodic peak in the same conditions.

be 120 mV s^{-1}.

$$\left(\frac{d \log I}{d\, Ni^{2+}}\right)_{pH,E} = +1.0$$

$$\left(\frac{d \log I}{d\, pH}\right)_{Ni^{2+},E} = +0.6$$

$$\left(\frac{d \log E}{dI}\right) = 0.12$$

The cathodic peak current function decreased with the square root of the scan rate and $I_p/v^{1/2}C_0$ decreased with increase in metal ion concentration (Fig. 2(b) and (c)) indicating the existence of surface adsorption by $(NiOH)_{ads}$.

In the presence of boric acid, the cathodic current was doubled (Fig. 3) and the peak potential shifted to more negative values. The deposit obtained was fine, smooth and semibright with increased cathode efficiency. All the above facts confirmed the specific adsorption of boric acid on the electrode surface modifying the structure of the deposit, as well as catalysing the discharge [7]. The increase in peak current and the shift in peak potential may be attributed to the buffering action at the interface.

In the reverse cycle (Fig. 3) only a small peak was observed at −300 mV in the absence of boric acid which characterized the dissolution of β-nickel [5]. Addition of boric acid shifted this peak to about −200 mV corresponding to the dissolution peak of alpha-nickel. Alpha-nickel is a solid solution of hydrogen in nickel with an atomic ratio of (H/Ni) 0.03 whereas beta-nickel is formed by interstitial hydrogen atoms.

$$Ni^{2+} + OH^- \longrightarrow (Ni\text{–}OH)^+ \quad (1)$$

$$(Ni\text{–}OH)^+ + e^- \xrightarrow{r.d.s.} (Ni\text{–}OH)_{ads} \quad (2)$$

$$(Ni\text{–}OH)_{ads} + e^- \longrightarrow Ni + OH^- \quad (3)$$

3.2. *Zinc deposition*

Unlike nickel, zinc discharge occurred at a more negative potential where hydrogen evolution also started (Fig. 4). In addition, the hydrogen discharge peak was absent due to adsorption of $Zn(OH)_{ads}$ at the electrode surface. This was again confirmed by the decrease in $I_p/v^{1/2}$ with sweep rate and also in $I_p/v^{1/2}C_0$ with increasing zinc concentration (Fig. 2(d) to (f)).

$$\left(\frac{d \log E}{dI}\right) = 0.06$$

and

$$\left(\frac{d \log I}{d\, Zn^{2+}}\right)_{pH,E} = 1.0$$

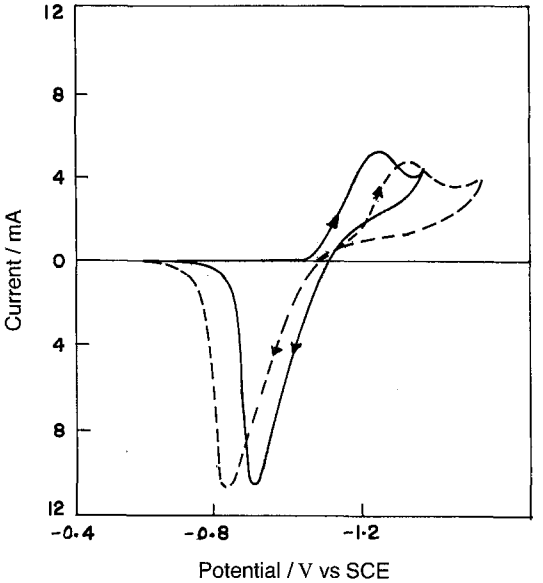

Fig. 4. CV in 0.5 M sodium sulfate (——) 0.1 M zinc sulfate, (– – –) 0.1 M zinc sulfate + 0.66 M boric acid, pH 3.2, 20 mV/s^{-1}.

The above facts supported a two step zinc discharge via $Zn(OH)_{ads}$ on a fraction of the electrode surface [8].

In the presence of boric acid the cathodic peak shifted to a more negative potential with a distinct hump at the foot of the voltammogram, which represented the hydrogen discharge reaction (Fig. 4). Hence, it was concluded that borate ions displaced a part of adsorbed zinc species, thereby hindering the discharge of zinc. The shift of the anodic peak potential towards more positive values confirmed that borate ions have a similar influence on the dissolution of zinc also.

3.3. *Zinc–nickel codeposition*

When 0.01 M zinc sulfate solution was added to 0.6 M nickel solution containing 0.66 M boric acid, a sudden increase in the peak current was observed accompanied by about 200 mV shift in the deposition potential towards more negative values (Fig. 5), due to the inhibition of nickel discharge by zinc ions. The increase in current is associated with simultaneous deposition of zinc and nickel. When Zn^{2+} concentration was increased to 0.02 M a shift of about 40 mV towards more noble potentials with considerable reduction in peak current, compared to 0.01 M zinc addition, was observed. This confirmed the suppression of the hydrogen evolution reaction, as well as inhibition of nickel discharge, by zinc ions. With 0.05 M zinc further shift towards more noble potentials and the presence of two distinct peaks were observed. Probably, this point represented codeposition of zinc with nickel as an alloy, the first peak corresponding to that of zinc and the second that of nickel. This was confirmed by the progressive increase in peak current with increasing zinc content. Another interesting behaviour noted at concentrations above 0.05 M was a shift in deposition potential towards less noble values. As explained by Lustman [9], the presence of the above two peaks indicate phase transformation during alloy deposition [10, 11].

With increasing zinc concentration the anodic peak became broader and active due to increase in zinc codeposition.

The two distinct peaks occurred only up to a Ni/Zn ratio of 5–6 and, below this, only a single peak was observed (Fig. 6). It is likely that the shift in peak potential for nickel deposition towards more negative values with decrease in its concentration in the electrolyte and associated hydrogen evolution has masked the nickel peak. It was also observed that the zinc deposition potential was not drastically altered by the progressive substitution by nickel ions, though addition of zinc ions, even in small amounts, to the nickel bath, altered the deposition potential of nickel.

When the potential was scanned in the anodic direction up to −1.40 V only a single peak appeared at about −400 mV, corresponding to the dissolution of nickel-rich alloy.

The peak current, however, increased progressively with increase in zinc content in the solution. The absence of multiple peaks denoting various phases of the deposit may be due to the formation of a nickel-rich alloy (alpha phase), at the diffusion limiting region of the second peak. However, when scanning was effected up to −1.2 V (Figs 7 and 8) anodic peaks corresponding to (i) alpha phase alloy and porous nickel, (ii) three peaks corresponding to gamma, alpha and porous nickel or (iii) two peaks corresponding to gamma and porous nickel were obtained at Ni/Zn

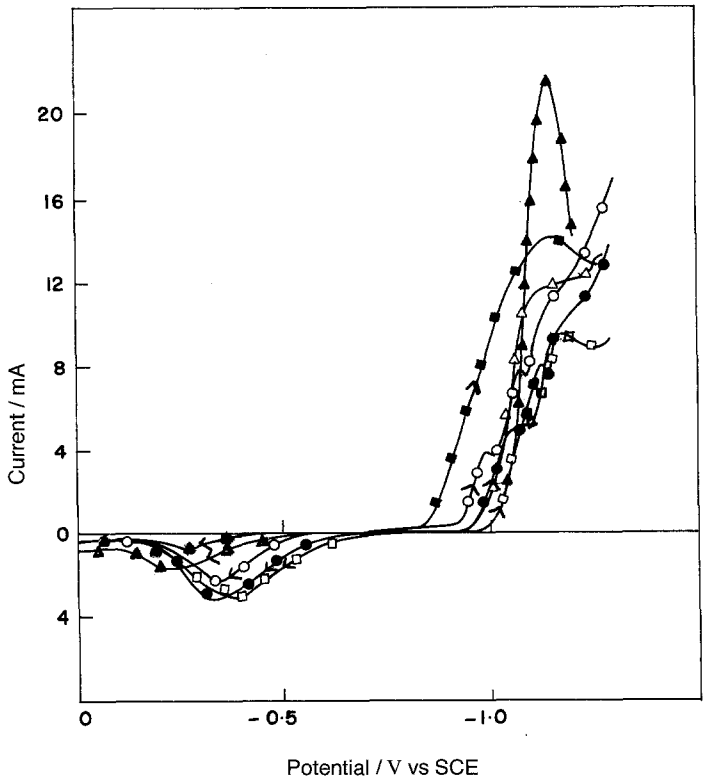

Fig. 5. CV showing the effect of zinc addition to a nickel electrolyte. Electrolyte: 0.5 M nickel sulfate, 0.66 M boric acid with zinc sulfate (M): (■) 0, (▲) 0.01, (△) 0.02, (○) 0.05, (●) 0.075, (□) 0.1, pH 3 10 mV s^{-1}.

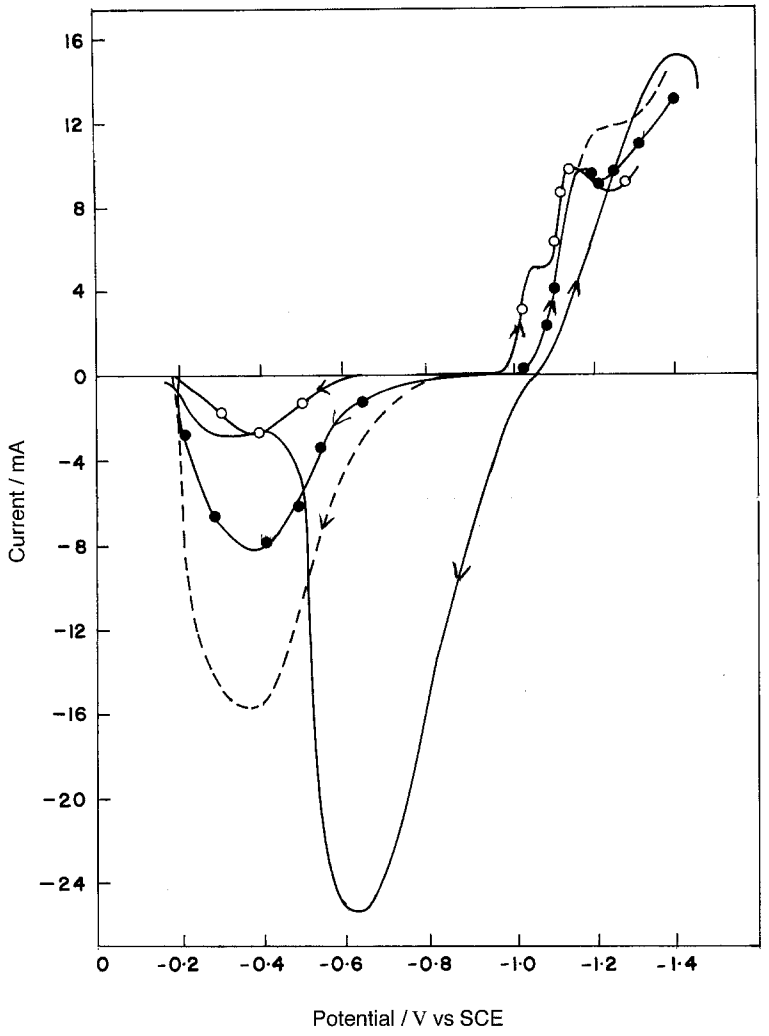

Fig. 6. CV showing the effect of Ni/Zn ratio. Electrolyte: 0.66 M boric acid, Ni/Zn: (○) 5, (●–●) 2, (– – –) 1, (——) 0.5 M zinc sulfate alone, pH 3, 10 mV s^{-1}.

ratios of 5, 2, 1 and 0.2, respectively [11–13]. The alpha phase is considered to be the phase transformation from the gamma phase during the dissolution process [11, 12].

Figure 9 shows the effect of scanning the potential up to −1300 mV. It was observed that the alpha phase is distinct and the nickel peak increases in the presence of boric acid, with a slight decrease in the gamma phase dissolution peak. This clearly indicates that boric acid favours nickel codeposition.

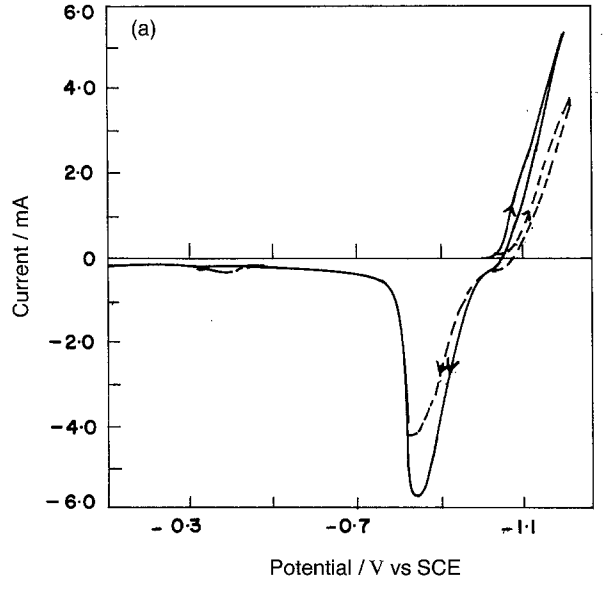

Fig. 7. CV showing the effect of Ni/Zn ratio on the dissolution peaks during alloy deposition. Ni/Zn ratio: (a) 0.2, (b) 1, pH 3, 10 mV s^{-1}, Scanning up to −1.2 V (——) without boric acid, (– – –) with boric acid.

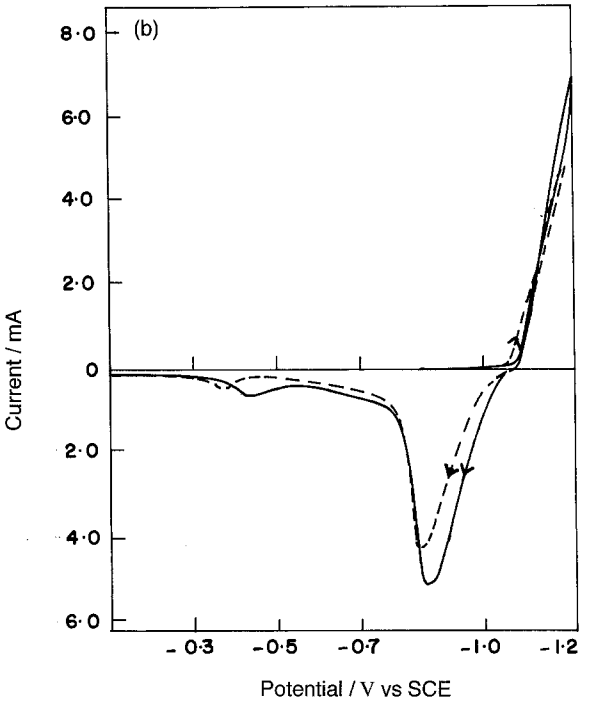

Fig. 7. Continued.

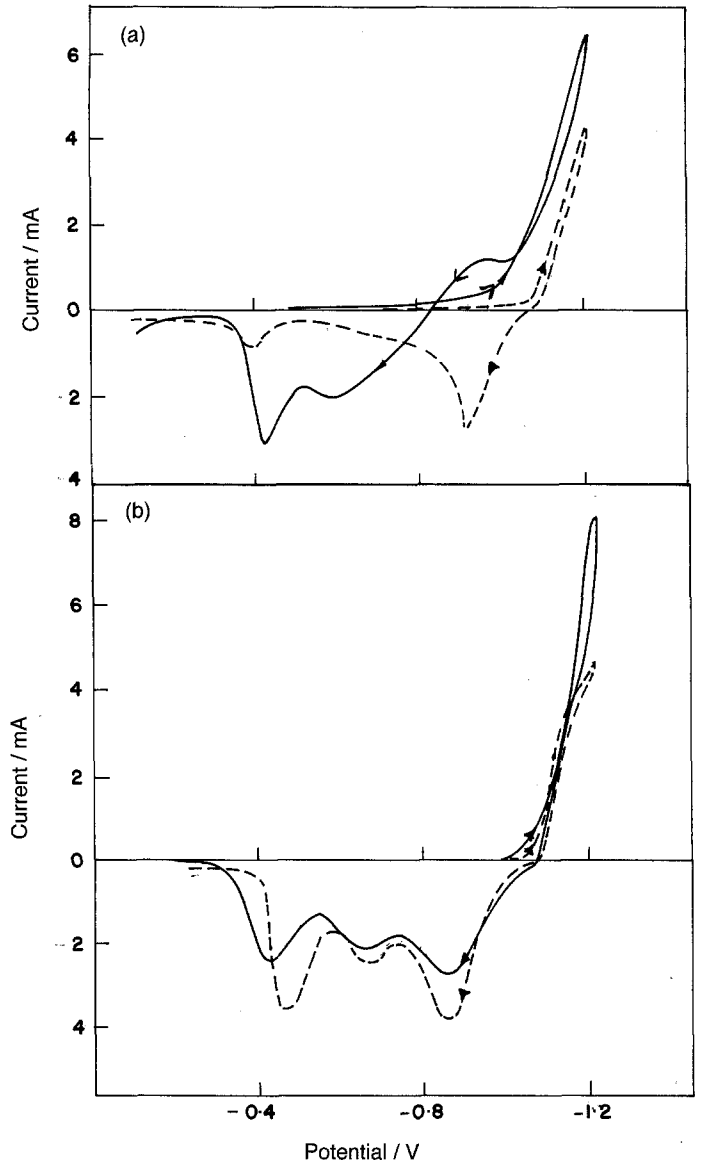

Fig. 8. CV as Fig. 7 with Ni/Zn ratio (a) 5, (b) 2.

When scanned up to −1080 mV (Fig. 10) only the zinc dissolution peak at about −1.0 V was observed. The stripping charge for a monolayer of zinc on nickel is about 460 μC cm^{-2} and the stripping charge obtained for this peak (120 μC) indicates only a monolayer coverage. When scanning up to about −1100 mV, the anodic part also showed the onset of a nickel peak. The charge calculated for this nickel dissolution peak (200 μC) corresponds to a few atomic layers of nickel [12]. From this it is clear that considerable inhibition to nickel deposition was caused by the presence of zinc ions. Above this potential, bulk zinc and nickel deposition was expected by which the adatoms may overcome the particle to particle repulsions to form clusters, which may not inhibit nickel deposition to the same extent as individually interacting adatoms. Also, at higher potentials the inhibition to nickel deposition caused by H^+ discharge diminished and more nickel may be codeposited with zinc.

As the potential was increased to more negative values, nucleation and growth of nickel becomes easier, resulting in a bulk alloy layer. The two stripping peaks moved closer indicating the formation of an intermediate phase (Ni_5Zn_{21}) [11]. The peak corresponding to alpha phase may be the result of phase transformations during dissolution of zinc in the gamma phase. At −1300 mV the anodic peak potential for the gamma phase became more noble with a decrease in peak current, indicating that, above this potential, alpha phase alloy was the dominant one.

These results indicate that during alloy deposition zinc ions are preferentially adsorbed at a faster rate than nickel ions, whose rate of reduction is also controlled by hydrogen codeposition. At higher potentials, both ions may interact forming a $(ZnNi)_{ads}$ layer, through which they deposit as the alloy. The composition of the alloys is decided by the number of sites occupied by each ion. Hence, it follows that the deposition mechanisms of the alloy is likely to be as follows:

$$H_2O \longrightarrow H^+ + OH^- \quad (4)$$

$$Zn^{2+} + OH^- \longrightarrow Zn(OH)^+ \quad (5)$$

$$Zn(OH)^+ + e^- \longrightarrow (ZnOH)_{ads} \quad (6)$$

$$(ZnOH)_{ads} + e^- \longrightarrow Zn + OH^- \quad (7)$$

$$(NiOH - ZnOH)_{ads} + 2e^- \longrightarrow NiZn + 2OH^- \quad (8)$$

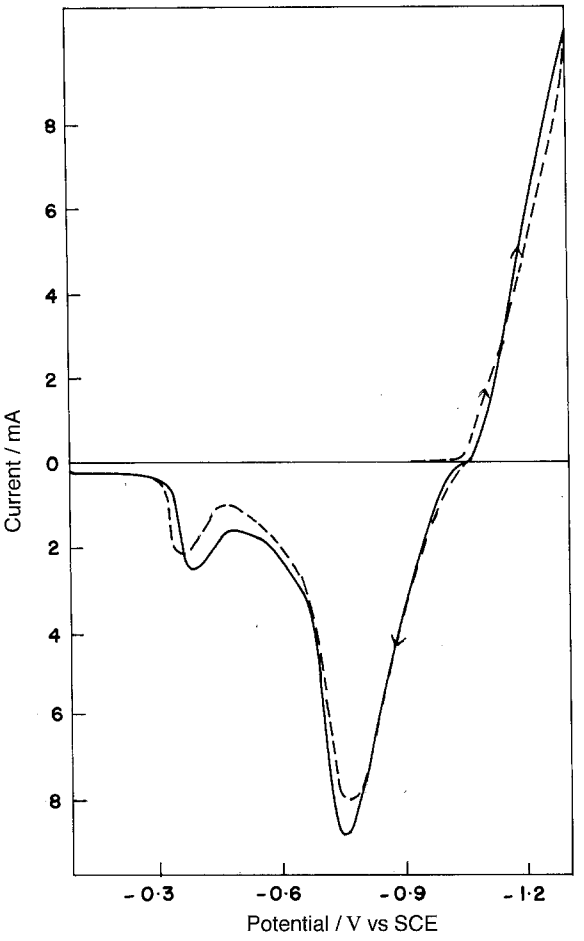

Fig. 9. CV showing the effect of boric acid on the dissolution peak of Ni–Zn deposition when scanned up to −1.30 V. Ni/Zn ratio 2, pH 3, 10 mV s^{-1}, (——) without boric acid, (– – –) with boric acid.

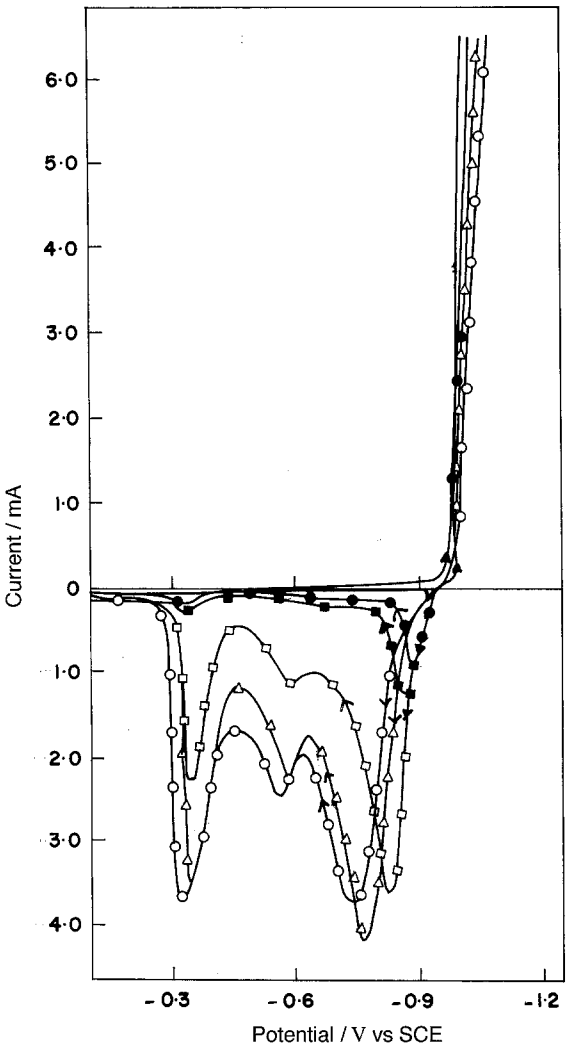

Fig. 10. Effect of varying the scan range from −100 mV to (– – –) −1080 mV, (●) −1100 mV, (■) −1150 mV, (□) −1200 mV, (△) −1250 mV, (○) −1300 mV. Ni/Zn ratio 2, pH 3, 10 mV s^{-1}.

Figures 7, 8 and 9 also show the anodic stripping behaviour of alloy deposits in the absence of boric acid. It is reasonable to assume that, with increasing nickel content, the hydrogen overpotential should decrease. When the Ni/Zn ratio was 5 the sites occupied by H^+ may be more numerous than those occupied by adsorbed zinc ions and hence deposition occurs in the alpha-phase, nickel being deposited in the beta-phase. Hence a broad anodic peak, indicating the formation of the solid solution followed by a porous beta-nickel layer, was observed. A negligible amount of zinc was also stripped from the alpha-phase alloy during reverse cycling with a cathodic current.

The presence of boric acid, due to its specific adsorption in the sites available for H^+, minimized Ni–H formation, resulting in considerable reduction in the Ni anodic peak current. Also, the presence of boric acid increased the deposition potential by 100 mV in the cathodic direction, favouring zinc deposition. When the Ni/Zn ratio was increased to 2, three distinct peaks corresponding to gamma, alpha and porous nickel were observed. In the presence of boric acid the peaks became closer, with an increase in peak current due to the larger active area of the components in the intermediate phase. With a Ni/Zn ratio of 1, the gamma-phase is large, with a small peak for nickel indicating a high zinc content. The presence of boric acid suppressed both the peaks, but to a greater extent than that of zinc. When the ratio was 0.2, in the absence of boric acid only, a dissolution peak of gamma-phase alloy was observed. But in the presence of boric acid the peak for porous

Table 1. Dependence of anodic charge on Zn^{2+} mole fraction for solutions without and with 0.66 M boric acid

Zinc mole fraction in the electrolyte	*Without H_3BO_3*/mC	*Anodic charge with H_3BO_3*/mC
0.16	8.64	5.11
0.33	12.60	9.28
0.50	9.15	7.5
0.80	8.17	6.60

Table 2. Dependence of peak current P_{a1} on the Zn^{2+} mole fraction in the electrolyte without and with boric acid

Zinc mole fraction in the electrolyte	*Peak current without H_3BO_3* /mA	*with H_3BO_3* /mA	*Reduction* /%
0.17	–	3.20	–
0.33	3.70	2.80	24.0
0.50	5.20	4.30	24.0
0.80	5.60	4.20	16.0

Table 3. Dependence of peak current P_{a3} on Zn^{2+} mole fraction in the electrolyte without and with boric acid

Zinc mole fraction in the electrolyte	*Peak current without H_3BO_3* /mA	*with H_3BO_3* /mA	*Increase* /%
0.16	1.20	1.70	42.0
0.33	1.00	1.90	90.0
0.50	0.20	0.40	100.0
0.80	0.20	0.45	100.0

nickel also appeared. The charges calculated for the Zn–Ni alloy deposition (Table 1) agree well with those of Karwas *et al.* [13]. The highest peak current for porous Ni dissolution at low Zn^{2+} concentration in the absence of boric acid could be due to hydrogen ionization. The peak currents (Tables 2 and 3) obtained for the Zn (a_1) and Ni (a_3) peaks reveal that boric acid suppresses Zn deposition more than nickel deposition.

4. Conclusion

The role of boric acid appears to be related to the H^+ discharge reaction. Whenever H^+ discharge increases beta-Ni formation is favoured. However, the formation of the latter is suppressed by boric acid by preferential adsorption on sites available for H^+. This enables deposition of Ni in the alpha-phase or as porous Ni with low hydrogen content. When H^+ discharge is increasingly low due to adsorption of Zn ions, boric acid (in low Ni/Zn ratios) suppresses Zn discharge by partly replacing adsorbed Zn ions with borate ions.

References

[1] M. Pushpavanam, V. Raman, S. Jayakrishnan and B. A. Shenoy, *Met. Finish.* **81** (1983) 85.
[2] M. Pushpavanam and K. Balakrishnan, *Met. Finish.*, submitted.
[3] *Idem, Trans. Inst. Metal Finish.*, in press.
[4] M. Pushpavanam, S. R. Natarajan and K. Balakrishnan, *J. Appl. Electrochem.* **21** (1991) 642.
[5] Yu. PO. Lin and J. R. Selman, *J. Electrochem. Soc.* **140** (1994) 1240.
[6] M. Fleishman and A. Saraby-Reintjes, *Electrochim. Acta* **29** (1984) 557.
[7] J. P. Hoare, *J. Electrochem. Soc.* **133** (1986) 2491.
[8] B. E. Conway, J. O. M. Bockris, E. Yeager, S. V. M. Khan and R. E. White (eds), 'Comprehensive Treatise of Electrochemistry', Vol. 7, Plenum, New York (1983).
[9] B. Lustman, *Trans. Electrochem. Soc.* **84** (1986) 2491.
[10] A. Brenner, 'Electrodeposition of Alloys', Vol. 2, Academic, New York (1963).
[11] S. Swathirajan, *J. Electrochem. Soc.* **133** (1986) 671.
[12] S. Swathirajan, *J. Anal. Chem.* **221** (1987) 211.
[13] C. Karwas and T. Hepal, *J. Electrochem. Soc.* **135** (1988) 839.